

# Inerter Nonlinearities and the Impact on Suspension Control

Fu-Cheng Wang and Wei-Jiun Su

**Abstract**—This paper discusses the nonlinear properties of Inerters and their impact on vehicle suspension control. The Inerter was recently introduced as an ideal mechanical two-terminal element which is a substitute for the mass element with the applied force proportional to the relative acceleration across the terminals. Until now, ideal Inerters have been applied to car, motorcycle and train suspension systems, in which significant performance improvement was achieved. However, due to the mechanical construction, some nonlinear properties of the existing mechanical Inerter models are noted. This paper investigates the Inerter nonlinearities, including friction, backlash and the elastic effect, and their influence on vehicle suspension performance. A testing platform is also built to verify the nonlinear properties of the Inerter model. It is shown from the results that the suspension performance is in general degraded by inerter nonlinearities. However, the overall suspension performance with inerters is still better than the traditional suspensions.

## I. INTRODUCTION

HERE are two well-known analogies between mechanical and electrical systems, namely the “force-voltage” and “force-current” analogies. In the “force-current” analogy, the spring, damper and mass of mechanical systems are analog to the inductor, resistor and capacitor of electrical systems. However, it is noted that one terminal of “mass” is always grounded, such that the electrical networks with ungrounded capacitors do not have a direct mechanical analogy with springs, dampers and masses. As a result, it potentially narrows the class of passive mechanical impedances which can be physically realized [1]. It was from the appreciation of the gap in the old analogy between mechanical and electrical networks that a new mechanical element, called *Inerter*, was proposed [2]. An Inerter is an ideal mechanical two-terminal element that is a substitute for the mass element in mechanical/electrical analogy, with the defining equation as follows:

$$F = b \frac{d(v_2 - v_1)}{dt}, \quad (1)$$

in which  $F$  is the applied force and  $b$  is inertance, while  $v_1$  and  $v_2$  are the velocities of the two terminals.

Manuscript received on August 22, 2007, and revised on February 2, 2008. This work was supported in part by the National Science Council of Taiwan under Grant 95-2218-E-002-030.

Fu-Cheng Wang is with the Mechanical Engineering Department of National Taiwan University, No. 1, Sec. 4, Roosevelt Road, Taipei 10617, Taiwan. (phone: +886-2-33662680; fax: +886-2-23631755; e-mail: fcw@ntu.edu.tw).

Wei-Jiun Su was with the Mechanical Engineering Department of National Taiwan University, Taipei, Taiwan. He is now a Sergeant in the Taiwanese Army, Tainan, Taiwan (e-mail: r93522827@ntu.edu.tw).

With the introduction of Inerters, all passive network impedance (admittance) can be mechanically realized by three mechanical elements - springs, dampers and inerters. Consequently, broader use of passive network impedance (admittance) is allowed to achieve better system performance. The first successful application of the Inerter was to road car suspension systems [1], where several combining layouts of inerters, dampers and springs were optimized with respect to various performance criteria. In [3], the optimization was further carried out by using the LMI (Linear Matrix Inequalities) method, in which all passive transfer functions with fixed order were optimized for various performance measurements. The resulting passive networks were then synthesized by the Bott-Duffin realization method. It was shown that the system performance can be further improved by allowing higher-order passive impedance, with the drawback of very complicated network synthesis. The second application of an Inerter was to the mechanical steering compensator of high-performance motorcycles [4], where a passive network containing an Inerter was used to replace a conventional steering damper to improve stability of the system in both “wobble” and “weave” modes. The third Inerter application was to train suspension systems [5], in which the Inerter was located in both the body-bogie and bogie-wheel connections. Significant performance improvement was achieved, especially when employing an inerter between the bogie and the wheel.

As a mechanical network element, the Inerter can be realized in various ways. Until now, two realizations of Inerters, namely the rack-pinion inerter and ball-screw inerter, have been presented [1, 3, 5]. Due to the mechanical construction, some inerter nonlinearities have been noticed [1, 6, 7]. In [1], the friction force and damping effect of the rack-pinion inerter were noted and used to simulate the frequency responses of a real Inerter model. It was pointed out that the experimental data matched better with the theoretical Inerter by considering friction forces. In [7], a ball-screw inerter model was considered with the backlash and elastic effect. The parameters were then adjusted by comparing the time responses of the theoretical and practical Inerter models. In [6], a buffer network was placed in series with an Inerter to remove the nonlinear spiking of the force signals from the hydraulic testing rig. Through this arrangement, the Inerter device behaves as a damper around the crossover frequency and as an ideal Inerter in the intermediate frequency range, while at low frequencies it is dominated by friction.

This paper proposes a nonlinear inerter model by considering three nonlinear properties, namely the friction,

backlash and elastic effect, and discusses their influence on vehicle suspension systems. It is arranged as follows: in Section II, three basic suspension layouts are introduced to evaluate the performance of the vehicle models. In Section III, a nonlinear Inerter model is proposed by considering three nonlinear properties. In Section IV, an experimental platform is built to verify the nonlinearities of a ball-screw Inerter. In sections V, nonlinear inerters are applied to the suspension analysis of a quarter-car model. It is shown that the suspension performance is slightly influenced by the Inerter nonlinearities. Finally, some conclusions are drawn in Section VI.

## II. VEHICLE SUSPENSION MODEL

### A. The Suspension Models

Three suspension layouts shown in Figure 1 are considered, where  $b$ ,  $c$  and  $k$  represent the inerter, damper and spring, respectively. Among them, S1 is the traditional suspension, while S2 and S3 are suspension models that employ ideal Inerters. It is noted that S2 is a basic parallel arrangement and S3 is a basic serial arrangement.

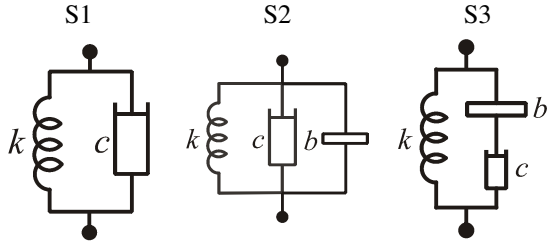


Figure 1. Suspension layouts for analysis.

### B. The Quarter-Car Model

A quarter-car model is illustrated in Figure 2 where  $Q$  represents the suspension layouts. The dynamics of this model can be described as follows:

$$m_s \hat{z}_s s^2 = \hat{F}_s - \hat{u}, \quad (2)$$

$$m_u \hat{z}_u s^2 = \hat{u} - \hat{F}_r, \quad (3)$$

where “ $\hat{\cdot}$ ” represents the Laplace transform of the corresponding variables, while the tyre force is  $\hat{F}_r = k_t(\hat{z}_u - \hat{z}_r)$  and the suspension force  $\hat{u}$  depends on the suspension layouts:

$$\text{For S1, } \hat{u} = (k + cs)(\hat{z}_s - \hat{z}_u),$$

$$\text{For S2, } \hat{u} = (k + cs + bs^2)(\hat{z}_s - \hat{z}_u),$$

$$\text{For S3, } \hat{u} = (k + \frac{bcs^2}{bs + c})(\hat{z}_s - \hat{z}_u).$$

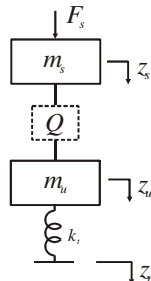


Figure 2. A general quarter-car model.

The system transfer function matrix can be represented as  $[\hat{z}_s \ \hat{z}_u]^T = G[\hat{F}_s \ \hat{z}_r]^T$ , in which  $G$  is a  $2 \times 2$  matrix. To measure the vehicle system performance, three performance indices are defined as follows [8]:

1).  $J_1$  (ride comfort)

$$J_1 = 2\pi\sqrt{(V\kappa)} \left\| \hat{T}_{\hat{z}_r \rightarrow \hat{z}_s} \right\|_2 = 2\pi\sqrt{(V\kappa)} \left\| s \hat{T}_{\hat{z}_r \rightarrow \hat{z}_s} \right\|_2, \quad (4)$$

2).  $J_3$  (dynamic tyre loads)

$$J_3 = 2\pi\sqrt{(V\kappa)} \left\| \hat{T}_{\hat{z}_r \rightarrow k_t(\hat{z}_u - \hat{z}_r)} \right\|_2 = 2\pi\sqrt{(V\kappa)} \left\| \frac{1}{s} \hat{T}_{\hat{z}_r \rightarrow k_t(\hat{z}_u - \hat{z}_r)} \right\|_2, \quad (5)$$

3).  $J_5$  (dynamic load carrying)

$$J_5 = \left\| \hat{T}_{\hat{F}_s \rightarrow \hat{z}_s} \right\|_\infty, \quad (6)$$

in which  $\hat{T}$  is the transfer functions with inputs and outputs in the subscripts, while  $V$  represents the driving velocity and  $\kappa$  is the road roughness parameter. The parameters are set as  $V = 25$  m/s and  $\kappa = 5 \times 10^{-7}$  m<sup>3</sup>cycle<sup>-1</sup> for performance analyses. It was shown in [1] that system performance can be improved (i.e. the performance indices can be reduced) by adopting inerters into the suspension design. For example, setting the parameters of  $m_s = 181.75$  kg,  $m_u = 25$  kg,  $k_t = 120$  kN/m [9] and optimizing the performance measures by tuning the values of inertance  $b$ 's and damping rates  $c$ 's, the performance improvement of the system is illustrated in Table 1. It is noted that the serial layout (S3) achieves better performance for  $J_1$  and  $J_3$ , while the parallel layout (S2) is better for  $J_5$ .

Table 1. Performance improvement of the quarter-car model ( $k = 120$  kN/m).

Layout	$J_1$	Improvement (%)	$c$ (Ns/m)	$b$ (kg)
S1	2.9882	0	4981	
S2	2.5773	13.75	3705.4	128.57
S3	2.4281	<b>18.745</b>	7544.2	366.52
Layout	$J_3$	Improvement (%)	$c$ (Ns/m)	$b$ (kg)
S1	598.52	0	4674.8	
S2	548.98	8.2764	3933	104.89
S3	501.20	<b>16.259</b>	6666.4	363.55
Layout	$J_5 (\times 10^{-5})$	Improvement (%)	$c$ (Ns/m)	$b$ (kg)
S1	3.8761	0	10230	
S2	2.0761	<b>46.436</b>	9301.3	328.34
S3	2.5946	33.061	11174	1232.4

## III. THE NON-LINEARITY OF INERTERS

Inerters can be mechanically realized in various ways. Until now, two types of Inerters, the rack-pinion inerter [1] and the ball-screw inerter [5, 6], have been presented. However, due to the mechanical construction, the nonlinearities of Inerter models need to be considered. In this section, three nonlinear properties of a ball-screw inerter, including the backlash, elastic effect and friction, are discussed and a nonlinear Inerter model is proposed. Furthermore, a testing platform is introduced to estimate the parameters of the inerter model by experiments.

### A. Backlash and the Elastic Effect

The ball-screw Inerter built by the *Mechanical Engineering Department of National Taiwan University (NTU-ME)* is illustrated in Figure 3. The working principle of the model is described as follows: two equivalent forces  $F$  are applied on the bearing and the nut such that the screw rotates with the flywheel. When the shaft is twisted by  $\theta$ , the nut has a translational displacement  $x = p \cdot (\theta / 2\pi)$ , where  $p$  (m/rev) is the pitch of the screw. Assuming the inertia of the flywheel is  $I$ , the ideal inertance of the model is  $b = I(2\pi / p)^2$ . As in the backlash and elastic effect of gears shown in [7, 10], the backlash  $\varepsilon$ , the elasticity  $k_s$  and viscous damping  $c_s$  of the ball-screw Inerter can also be considered in the axial direction, as shown in Figure 4.

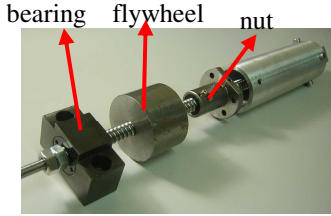


Figure 3. NTU-ME ball-screw Inerter.

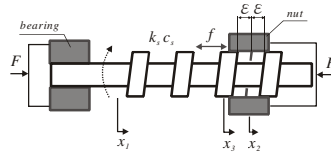


Figure 4. The Inerter nonlinearities.

The dynamic equations of the ball-screw Inerter are similar to those of the rotating model in [10]. Considering the displacement  $x$  in the axial direction, we define the compressed deformation as  $x_s = x_1 - x_3$ , the backlash displacement as  $x_b = x_3 - x_2$ , and the linear displacement between the two ports as  $x_d = x_1 - x_2$ . Therefore, the corresponding force  $F$  can be expressed as:

$$F(t) = k_s x_s + c_s \dot{x}_s = k_s (x_d - x_b) + c_s (\dot{x}_d - \dot{x}_b). \quad (7)$$

In the point of view of contact, three regions are given:

$$\begin{aligned} A_+ &= \{ (x_d, \dot{x}_d) : k_s x_d + c_s \dot{x}_d \geq k_s \varepsilon \}, \\ A_r &= \{ (x_d, \dot{x}_d) : |k_s x_d + c_s \dot{x}_d| < k_s \varepsilon \}, \\ A_- &= \{ (x_d, \dot{x}_d) : k_s x_d + c_s \dot{x}_d \leq -k_s \varepsilon \}. \end{aligned}$$

Three contact phenomena can be drawn from [10]:

- ◆ There can be persistent right contact (during a non-zero interval) only in  $A_+$  and persistent left contact only in  $A_-$ .
- ◆ If the system state  $(x_d, \dot{x}_d)$  at the initial time  $t = t_0$  lies in  $A_+$  with  $x_b(t_0) = \varepsilon$  (right contact), then  $x_b(t_1) = \varepsilon$  for all times  $t_1 > t_0$  such that  $(x_d(t), \dot{x}_d(t)) \in A_+$  for all  $t \in [t_0, t_1]$ . If  $(x_d(t_0), \dot{x}_d(t_0)) \in A_-$  with  $x_b(t_0) = -\varepsilon$  (left contact), then  $x_b(t_1) = -\varepsilon$  for all times  $t_1 > t_0$  such that  $(x_d(t), \dot{x}_d(t)) \in A_-$  for all  $t \in [t_0, t_1]$ .
- ◆ Assuming that  $x_b(t_0) = \varepsilon$  or  $x_b(t_0) = -\varepsilon$  and the trajectory  $(x_d(t_0), \dot{x}_d(t_0))$  reaches the release set  $A_r$ , contact is lost at the first time  $t_1 > t_0$ .

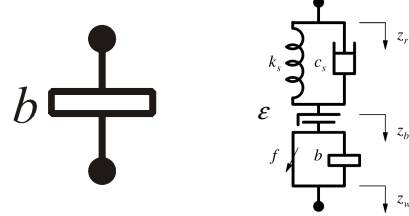
### B. Friction

Friction force exists in the contact surfaces. In order to reduce the friction, devices are often lubricated to reduce the

roughness of the contact surfaces. For the gear motion, friction happens in the contact of the teeth. For the ball-screw, the contact between the nut and screw threads is normally considered as rolling contact with a small friction coefficient [11]. However, for the application of suspension systems, the friction force is not negligible because the normal force on the contact surfaces is significant by preloading.

### C. Inerter Model with Nonlinear Properties

Considering the aforementioned three nonlinearities, a nonlinear Inerter model is proposed in Figure 5(b) where  $c_s$  and  $k_s$  represent the elastic effect, while  $\varepsilon$  is the backlash and  $f$  is the friction force.



(a) An ideal Inerter. (b) A non-linear Inerter.  
Figure 5. The ideal and non-linear Inerter models.

## IV. EXPERIMENTAL DESIGN AND RESULTS

### A. Testing Platform

The testing platform is a motion table with one degree of freedom which is driven by a servo motor to control the displacement of the suspension strut, as shown in Figure 6. The force of the device is measured by an S-type load cell with the maximum load of 100 kg and resolution of 0.02 kg, while the displacement is measured by a position encoder with an accuracy of 1  $\mu\text{m}$ . Both of the force and displacement signals are acquired through a LabView<sup>TM</sup> program.

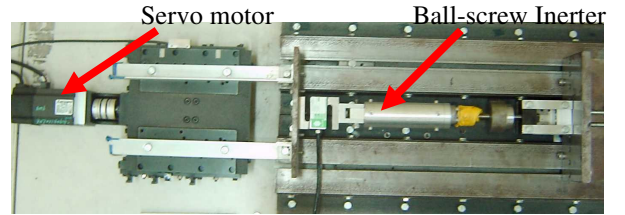


Figure 6. The experiment platform.

### B. Parameter Estimation of the Nonlinear Inerter

We established the nonlinear Inerter model in Simulink<sup>TM</sup> and compared the theoretical force output with the experimental data, in order to estimate the parameters of the nonlinear Inerter. For the experimental strut, the inertance of the ball-screw shaft without the flywheel was 5 kg. A flywheel with corresponding inertance of 108 kg was then installed for test such that the total inertance is 113 kg. The parameters  $k_s$ ,  $c_s$ ,  $\varepsilon$  and  $f$  were tuned by the least-squares steepest descent optimization algorithm [6] as follows:

$$\min_{k_s, c_s, \varepsilon, f} \left\| (f_{th}(k_s, c_s, \varepsilon, f) - f_{exp}) \right\|_2^2, \quad (8)$$

where  $f_{exp}$  is the force measured from the experiments, and  $f_{th}$  is the force calculated from the theoretical non-linear model.

In order to measure the friction  $f$ , the flywheel is uninstalled. The friction force  $f$  can then be measured by giving a low frequency sinusoidal input. Because the Inerter force is negligible in this case, the measured force accounts mainly for the friction. Setting the input as a cosine wave of 0.1 Hz with amplitude of 1mm, the measured displacement and force are shown in Figure 7. It is noted that the friction  $f$  is almost a square wave, with the amplitude of about 10 N and the direction opposite to the sign of the velocity. Considering the nonlinear Inerter model of Figure 5(b), the size of the friction  $f$  can be regarded as constant for the theoretical model such that (7) can be rearranged as:

$$c_s(\dot{z}_r - \dot{z}_b) + k_s(z_r - z_b) = b(\ddot{z}_b - \ddot{z}_w) + f_c \cdot \text{sign}(\dot{z}_b - \dot{z}_w), \quad (9)$$

where  $f_c=10\text{N}$ .

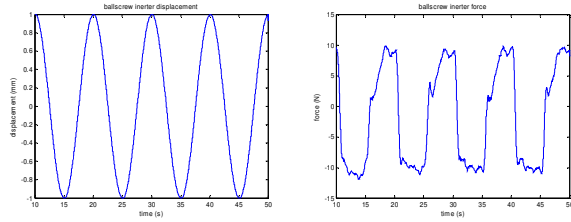


Figure 7. The displacement and force signals of the Inerter.

Given an input  $r = \cos(6\pi t)$ , the parameters  $k_s$ ,  $c_s$  and  $\varepsilon$  can be tuned to match the experimental data, as shown in Figure 8. Using the optimization algorithm of (8), the best fit between the experimental and the theoretical data is taken as follows:  $k_s = 1000 \text{ kN/m}$ ,  $c_s = 3200 \text{ Ns/m}$  and  $\varepsilon = 0$ .

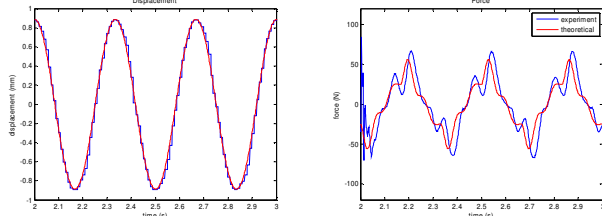


Figure 8. Tuning of the nonlinear parameters ( $b=113\text{kg}$ ).

From the optimization results, there is no backlash in the ball-screw Inerter. The reason is that the ball-screw set is normally preloaded to eliminate backlash in the manufacturing process. Some preloading methods, such as the double nut preloading and oversized-ball preloading, are described in [12].

## V. THE IMPACT ON VEHICLE SUSPENSION CONTROL

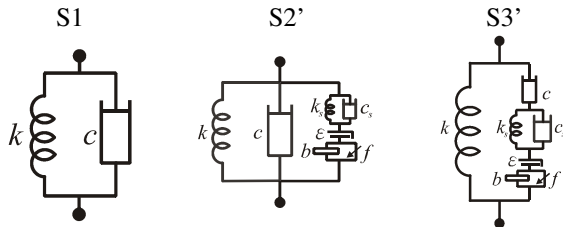


Figure 9. Suspension models with nonlinear Inerters.

In this section, the nonlinear Inerter model is applied to the performance analyses of the quarter-car suspension systems. Compared to the three suspension layouts of Figure 1 with linear inerters, there are three kinds of suspension models in consideration, as shown in Figure 9

### A. The Analysis Methods

For linear systems, the performance can be evaluated by directly calculating the  $H_2$  and  $H_\infty$  norms of the system transfer functions. But for nonlinear systems, it can not be directly obtained because the transfer functions are time-varying and depend on the input. In order to analyze the system performance with nonlinear Inerter, time domain responses are used. That is, a suitable input  $z_r$  with the spectral density of  $S^{z_r}(f) = \kappa V / f^2$  [1] is generated to simulate responses of the nonlinear system. Then the performance indices are calculated by taking the expected values of the outputs. That is, the *r.m.s. body vertical acceleration discomfort parameter* is  $J_1 = \sqrt{E[\dot{z}_s^2(t)]}$ , and the *r.m.s. dynamic tyre load parameter* is  $J_3 = \sqrt{E[F_r^2(t)]}$ , in which  $F_r = k_t(z_r - z_u)$ .

The input signal to calculate  $J_1$  and  $J_3$  is  $z_r$ . Considering the spectral density of the road input  $S^{z_r}(f) = \kappa V / f^2$  [1],  $z_r$  is constructed by the following time sequence:

$$z_r = \sum_{i=1}^N A_i \sin(\omega_i t + \theta), \quad (10)$$

where  $N$  is the number of frequency points. The magnitudes are taken as  $A_i = \sqrt{8\pi\kappa V \cdot \Delta\omega_i} / \omega_i$ , in which  $\Delta\omega_i = \omega_{i+1} - \omega_i$  and  $\Delta\omega_N = \Delta\omega_{N-1}$ , and the phase  $\theta$  is random such that the spectral density of  $z_r$  is close to  $\kappa V / f^2$ . In the simulation, the frequency points  $\omega_i$  are set between 0.1 Hz and 1000 Hz with intervals of 0.1 Hz, i.e.  $\omega_i = [0.1, 0.2, 0.3, \dots, 1000]$  Hz. An input signal generated from (10) is illustrated in Figure 10. To verify the accuracy of this method, the performance indices of the linear systems are evaluated by this method and compared with the direct calculation of system norms. The results are shown to match with each other.

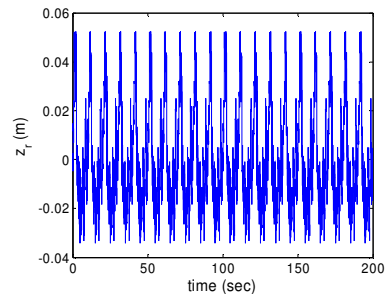


Figure 10. Input signal of the expected-value method.

For  $J_5$ , the input signal is  $F_s$ . It is noted that the performance index  $J_5$  represents the dynamic load carrying as in (6), which can be regarded as the induced 2-norm of the systems, i.e.

$$J_5 = \left\| T_{\hat{F}_s \rightarrow \hat{z}_s} \right\|_\infty = \sup_{\hat{F}_s \neq 0} \frac{\|\hat{z}_s\|_2}{\|\hat{F}_s\|_2} = \sup_{F_s \neq 0} \frac{\|z_s\|_2}{\|F_s\|_2}, \quad (11)$$

where the last equivalence is from the Parseval's Relations [13]. That is, the performance index is considered as the maximum ratio of the output energy to the input energy. Firstly, the peak frequency  $\omega_0$  where the infinity norm of the linear system occurs is found. Then, for the nonlinear systems, the input signal is taken as  $F_s = A \sin(\omega t)$ , in which we set  $A = 1000$  N for the quarter-car model and  $A = 2000$  N for the half-car model. Then we search the nearby frequency by setting  $\omega \approx \omega_0$  to simulate the output responses in order to numerically find the maximum energy ratio by (11).

### B. Inerter with the Elastic Effect Only

To consider the impact of the elastic effect, two settings of  $k_s$  and  $c_s$  are applied to illustrate their influence on suspension performance. The first is from the experimental results of Section IV, where  $k_s = 1000$  kN/m,  $c_s = 3200$  Ns/m. The second is twice harder with  $k_s = 2000$  kN/m,  $c_s = 6400$  Ns/m. It is noted that an ideal Inerter can be considered as when  $k_s$  and  $c_s$  are infinity. Referring to Figure 5(b), Inerter with only the elastic effect can be regarded as a linear model in which an ideal inerter is in series with a parallel spring/damper set, such that the best achievable performance can be re-optimized for this model.

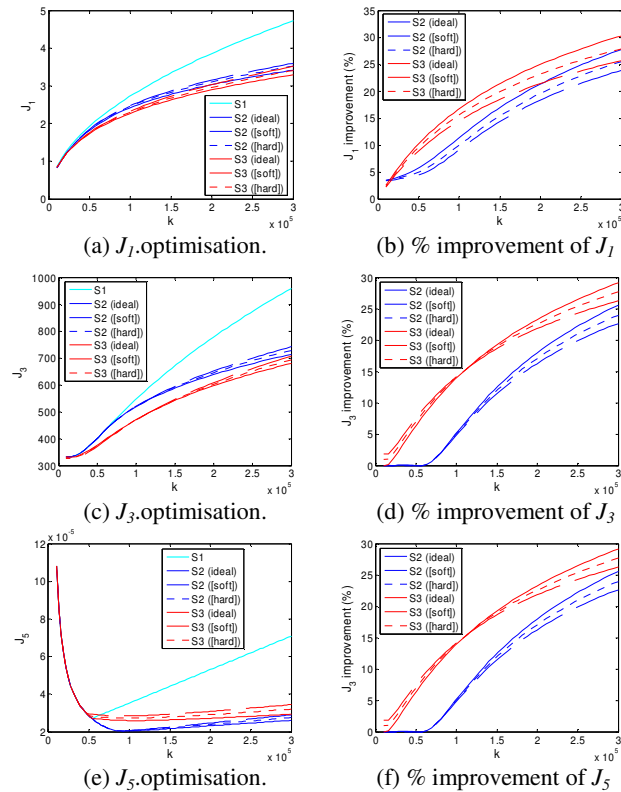


Figure 11. Performance optimizations of the quarter-car model employing inerters with the elastic effect.

The performance optimization is shown in Figure 11. For  $J_1$ , the results are shown in Figure 11(a)(b), where the performance benefit decreases with the elastic effect. And the

softer the elastic settings are, the more is the performance reduction. For  $J_3$  the results are slightly different from  $J_1$ , as illustrated in Figure 11(c)(d). For the serial arrangement (S3) the performance improvement is slightly increased when  $k$  is smaller than 120 kN/m. Apart from that, the suspension performance is in general degraded by the elastic effect. For  $J_5$ , the results are shown in Figure 11(e)(f). It is noted that the softer shaft has less performance benefits. Note that the serial arrangement (S3) with elastic effect is even worse than the traditional suspension (S1) when  $k$  is about 55 kN/m.

Table 2. Performance optimization of the quarter-car model employing frictional Inerter ( $k = 120$  kN/m).

	Case	Layout	$c$ (Ns/m)	$b$ (kg)	$J$ (ideal)	Expectation	Improv. (%)
$J_1$	1	S1	4981		2.9882	2.9878	0
	2	S2	3705.4	128.57	2.5573	2.5885	<u>13.364</u>
	3	S2( $f=10$ N)	3705.4	128.57		2.5878	13.389
	4	S2( $f=100$ N)	3705.4	128.57		2.6188	12.352
	5	S3	7544.2	366.52	2.4281	2.4293	<u>18.694</u>
	6	S3( $f=10$ N)	7544.2	366.52		2.4355	18.485
	7	S3( $f=100$ N)	7544.2	366.52		2.5000	16.326
$J_3$	1	S1	4674.8		598.52	601.13	0
	2	S2	3933	104.89	548.98	522.07	<u>8.162</u>
	3	S2 ( $f=10$ N)	3933	104.89		551.90	8.190
	4	S2 ( $f=100$ N)	3933	104.89		557.98	7.179
	5	S3	6666.4	363.55	501.20	504.65	<u>16.050</u>
	6	S3( $f=10$ N)	6666.4	363.55		506.07	15.815
	7	S3 ( $f=100$ N)	6666.4	363.55		519.76	13.537
$J_5$	1	S1	10230.2		$3.8761 \times 10^{-5}$	$3.8686 \times 10^{-5}$	
	2	S2	9301.3	328.34	$2.0761 \times 10^{-5}$	$2.0736 \times 10^{-5}$	<u>46.399</u>
	3	S2 ( $f=10$ N)	9301.3	328.34		$2.0848 \times 10^{-5}$	46.110
	4	S2 ( $f=100$ N)	9301.3	328.34		$2.1869 \times 10^{-5}$	43.471
	5	S3	11174.5	1232.42	$2.5946 \times 10^{-5}$	$2.5924 \times 10^{-5}$	<u>52.989</u>
	6	S3( $f=10$ N)	11174.5	1232.42		$2.5866 \times 10^{-5}$	33.139
	7	S3 ( $f=100$ N)	11174.5	1232.42		$2.5396 \times 10^{-5}$	34.354

### C. Inerter with Friction Only

Setting the suspension stiffness  $k = 120$  kN/m, the impact of friction on performance is illustrated in Table 2, where cases 1, 2, 5 are with ideal suspension elements and cases 3, 4, 6, 7 are with frictional inerters. To emphasize the influence of friction force on the performance, a much larger friction force  $f=100$  N is used to compare with the experimental setting  $f=10$  N. The expected values of  $J_1 = \sqrt{E[\ddot{z}_s^2(t)]}$  are the average of

four simulations. First of all, for accurate comparison, the expected values of the linear models (cases 1, 2, 5) are compared with the direct calculations of the system norms. It is shown that the errors are within 1%, so that the expected value is a reliable performance index. For the analyses of  $J_1$ , it is noted that the performance variation is relatively ignorable when the friction is small (cases 3 and 6). But when the friction is large (cases 4 and 7), the performance decrease is obvious. For  $J_3$ , the influence of friction is similar. When the friction is small (10 N), the influence on the performance is almost negligible. But when the friction is large (100 N), the performance degrades about 1% for S2 and 2.5% for S3 layouts. For  $J_5$ , in the linear systems (cases 1, 2, and 5),  $J_5$  is calculated from both the theoretical  $H_\infty$  norm of (6) and the

energy ratio of (11) to illustrate the accuracy of this method. It is shown that the performance is decreased by friction for the parallel arrangement, and slightly improved for the serial arrangement (cases 3 and 6). The tendency is more obvious with larger friction settings (cases 4 and 7).

*D. Inerters with both the Friction and Elastic Effect*

Considering both the inerter friction and elastic effect, the impact of Inerter nonlinearities on performance when  $k = 120\text{kN/m}$  is illustrated in Table 3. In which cases 1, 2, 6 are suspension models with ideal inerters, and cases 3, 7 are suspension models with inerters applying the elastic effect ( $k_s = 1000\text{kN/m}$ ,  $c_s = 3200\text{Ns/m}$ ), and cases 4, 8 are suspension models with inerters applying friction ( $f=10\text{ N}$ ), and cases 5, 9 are the suspension models with inerters applying both friction and the elastic effect. For  $J_1$ , it is shown that the performance is much more influenced by the elastic effect than friction, and the overall performance is degraded by Inerter nonlinearities by 2-3%. For  $J_3$ , the influence of Inerter nonlinearities is less significant, with the overall degradation of about 0.5%. For  $J_5$ , the performance is in general decreased by the elastic effect (cases 3 and 7), but slightly improved by friction for the serial arrangement (S3).

Table 3. Performance optimization of the quarter-car model employing Inerter with both of the friction and elastic effect ( $k = 120\text{ kN/m}$ ).

	Case	Layout	$c$ (Ns/m)	$b$ (kg)	$J$ (ideal)	Expectation	Impro. (%)
$J_1$	1	S1	4981		2.9882	2.9878	
	2	S2	3705.4	128.57	2.5773	2.5885	13.364
	3	S2(elastic)	3834.4	110.84	2.6488	2.6492	11.332
	4	S2(friction)	3705.4	128.57		2.5878	13.389
	5	S2(both)	3834.4	110.84		2.6482	11.366
	6	S3	7544.2	366.52	2.4281	2.4293	18.694
	7	S3(elastic)	7353	328.72	2.5027	2.5039	16.198
	8	S3(friction)	7544.2	366.52		2.4355	18.485
	9	S3(both)	7353	328.72		2.5103	15.981
$J_3$	1	S1	4674.8		598.52	601.13	0
	2	S2	3933	104.89	548.98	552.07	8.162
	3	S2(elastic)	3955.8	93.198	552.50	555.54	7.585
	4	S2(friction)	3933	104.89		551.90	8.190
	5	S2(both)	3955.8	93.198		555.11	7.657
	6	S3	6666.4	363.55	501.20	504.65	16.050
	7	S3(elastic)	6736.6	325.42	501.94	505.38	15.929
	8	S3(friction)	6666.4	363.55		506.07	15.815
	9	S3(both)	6736.6	325.42		506.80	15.692
$J_5$	1	S1	10230.2		$3.8761 \times 10^5$	$3.8686 \times 10^5$	0
	2	S2	9301.3	328.34	$2.0761 \times 10^5$	$2.0736 \times 10^5$	46.399
	3	S2(elastic)	9374.5	271.71	$2.1238 \times 10^5$	$2.1228 \times 10^5$	45.127
	4	S2(friction)	9301.3	328.34		$2.0848 \times 10^5$	46.110
	5	S2(both)	9374.5	271.71		$2.1123 \times 10^5$	45.399
	6	S3	11174.5	1232.42	$2.5946 \times 10^5$	$2.5924 \times 10^5$	32.989
	7	S3(elastic)	10174.3	888.29	$2.8606 \times 10^5$	$2.8571 \times 10^5$	26.146
	8	S3(friction)	11174.5	1232.42		$2.5866 \times 10^5$	33.139
	9	S3(both)	10174.3	888.29		$2.8584 \times 10^5$	26.113

VI. CONCLUDING REMARKS

This paper has proposed a nonlinear Inerter model to consider three nonlinear properties of a mechanical ball-screw

inerter, and discussed their impact on vehicle suspension control. From the experimental results, it was shown that a ball-screw Inerter has both of the elastic effect and friction. The nonlinear Inerter was then applied to vehicle suspension design. The individual and combined effects of Inerter nonlinearities were discussed in three scenarios. From the results, it was shown that the suspension performance was in general degraded by Inerter nonlinearities, except for the elastic effect in S3 model where  $J_3$  was slightly increased when the suspension stiffness  $k$  is small. However, even with the slightly influence of Inerter nonlinearities, it was illustrated that the overall suspension performance with nonlinear Inerter is still better than the traditional suspensions, especially when the suspension stiffness  $k$  is large.

REFERENCES

- [1]. M.C. Smith and F.C. Wang, "Performance Benefits in Passive Vehicle Suspensions Employing Inerters." *Vehicle System Dynamics* 42 (4), pp. 235-257, 2004.
- [2]. M.C. Smith, "Synthesis of Mechanical Networks: The Inerter." *IEEE Transactions on Automatic Control*, 47, pp. 1648-1662, 2002.
- [3]. C. Papageorgiou and M.C. Smith, "Positive Real Synthesis Using Matrix Inequalities for Mechanical Networks: Application to Vehicle Suspension" *IEEE Trans. on Contr. Syst. Tech.* 14 (3), pp. 423-435, 2006.
- [4]. S. Evangelou, D.J.N. Limebeer, R.S. Sharp, and M.C. Smith, "Steering Compensation for High-Performance Motorcycles", *Proceedings of the 43rd IEEE Conference on Decision and Control*, pp. 749-754, Paradise Island, Bahamas, 14-17 Dec. 2004.
- [5]. F.C. Wang, C.H. Yu, Mong-Lon Chang and Mowson Hsu, "The Performance Improvements of Train Suspension Systems with Inerters", *Proceedings of the 45th IEEE Conference on Decision and Control*, pp. 1472-1477, San Diego, CA, USA, 13-15 Dec. 2006.
- [6]. C. Papageorgiou. and M.C. Smith, "Laboratory Experimental Testing of Inerters." *44th IEEE Conference on Decision and Control*, 2005 and 2005 European Control Conference. CDC-ECC '05, pp. 3351 - 3356, 12-15 Dec. 2005.
- [7]. C. Papageorgiou, "Analysis of experimental data from the testing of inerter devices", *Technical Report: F-INFENG/TR.524*, Control Group, Department of Engineering, University of Cambridge, 2005.
- [8]. M.C. Smith and G.W. Walker, "A Mechanical Network Approach to Performance Capabilities of Passive Suspensions", *Proceedings of the Workshop on Modeling and Control of Mechanical Systems*, pp. 103-117, Imperial College, London, 17-20 June 1997.
- [9]. J.C. Dixon, "Tyres, Suspension and Handling", Cambridge University Press, first edition, 1991.
- [10]. M. Nordin, J. Galic and P.O. Gutman, "New Models for Backlash and Gear Play", *International Journal of Adaptive Control and Signal Processing* (11), pp. 49-63, 1997.
- [11]. R.L. Norton, "Machine Design. An integrated Approach", Prentice-Hall, Second edition, 2000.
- [12]. Catalog of NSK ballscrew. Precision Machine Components. CAT.No.E3161a.
- [13]. K. Zhou, J.C. Doyle and K. Glover, "Robust and Optimal Control", Prentice-Hall, 1996.